STANFORD
AERONAUTICS &
ASTRONAUTICS

AA200
Applied Aerodynamics

Chapter 5 - Kinematics of fluid motion

STANFORD
AERONAUTICS &
ASTRONAUTICS

Steady flow pattern in the wake of a circular cylinder.

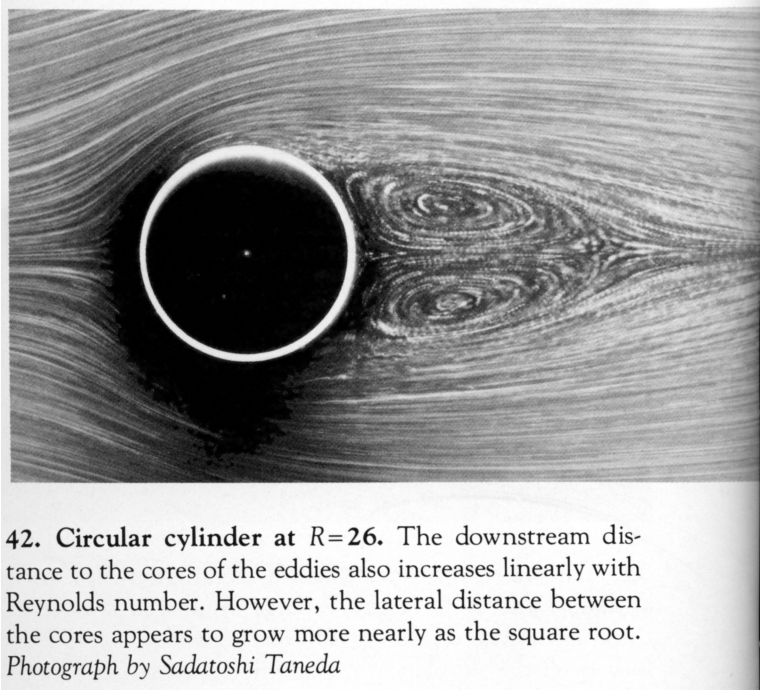

42. Circular cylinder at $R=26$. The downstream distance to the cores of the eddies also increases linearly with Reynolds number. However, the lateral distance between the cores appears to grow more nearly as the square root. *Photograph by Sadatoshi Taneda*

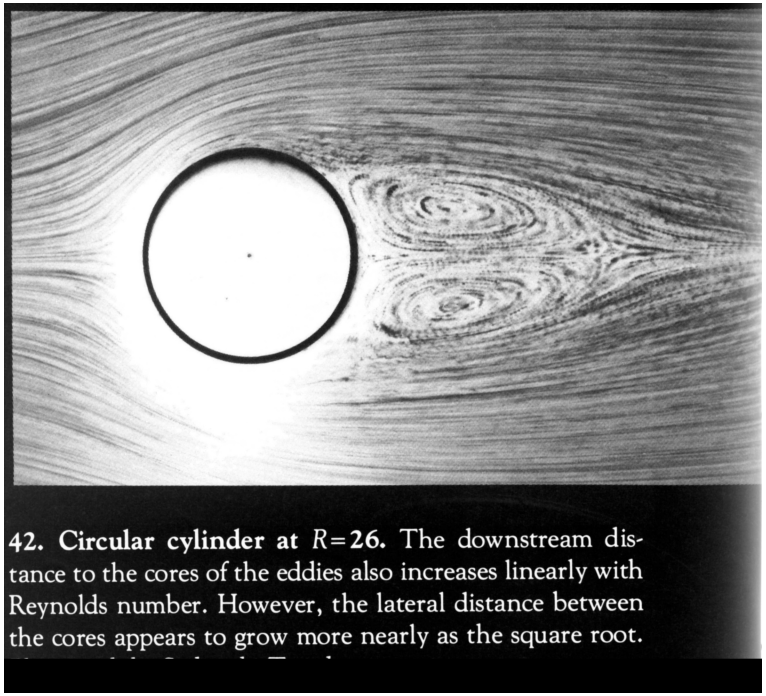

42. Circular cylinder at $R=26$. The downstream distance to the cores of the eddies also increases linearly with Reynolds number. However, the lateral distance between the cores appears to grow more nearly as the square root.

STANFORD
AERONAUTICS &
ASTRONAUTICS

Surface flow patterns.

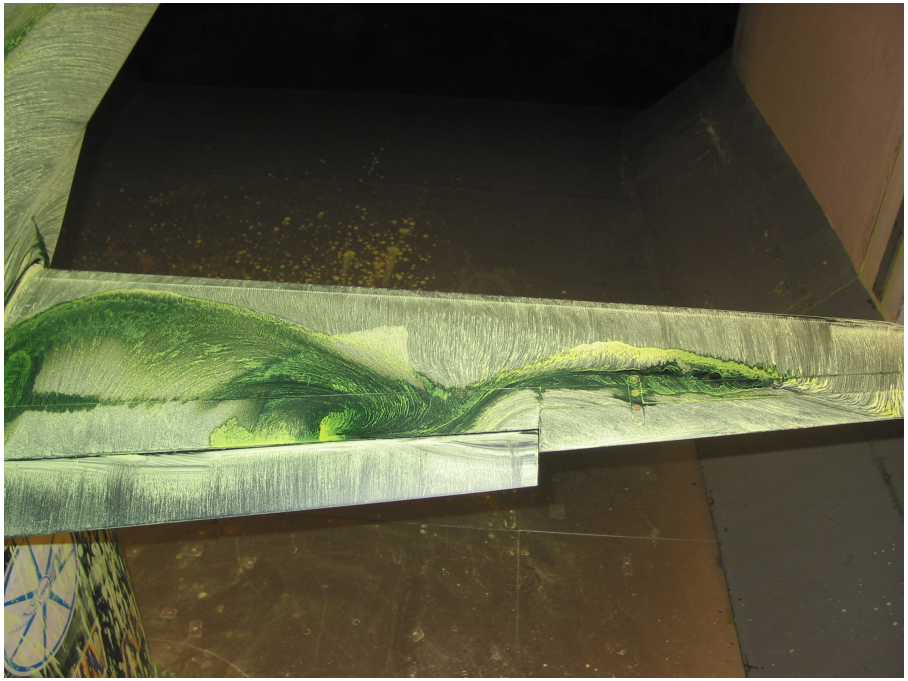

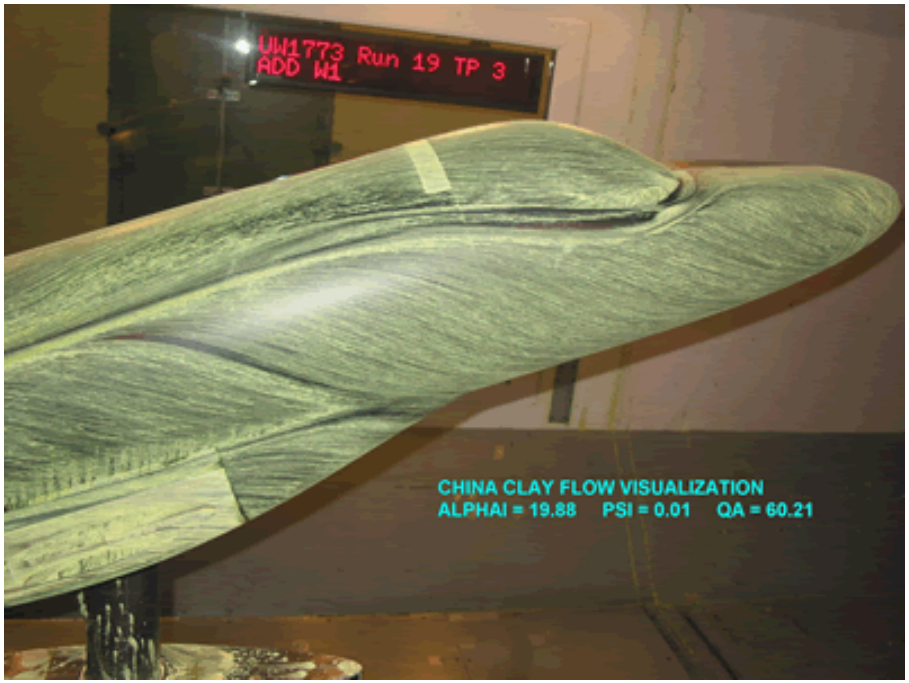

STANFORD
AERONAUTICS &
ASTRONAUTICS

4.1 Elementary flow patterns

Let's return to the equations for particle paths in a steady flow.

$$\frac{dx}{dt} = U(\bar{x}) ; \qquad \frac{dy}{dt} = V(\bar{x}) ; \qquad \frac{dz}{dt} = W(\bar{x}) .$$

A lot about the flow can be learned by plotting the velocity field. Critical points occur where the velocity is zero.

$$U_i[\boldsymbol{x}_c] = 0 .$$

Reference:

CHONG, M. S., PERRY, A. E. and CANTWELL, B. J. 1990 A general classification of three-dimensional flow patterns. *Physics of Fluids* A Vol. **2** (5): 765-777.

STANFORD
AERONAUTICS &
ASTRONAUTICS

Linear flows

Assume the velocity field is an analytic function of position. Then the velocity field can be expanded in a Taylor series about any point in the flow. Near a critical point

$$\frac{dx_i}{ds} = A_{ik}(x_k - x_{kc}) + O((x_k - x_{kc})^2) + \ldots$$

where

$$A_{ik} = \left(\frac{\partial U_i}{\partial x_k}\right)_{\boldsymbol{x} = \boldsymbol{x}_c}.$$

is the velocity gradient tensor evaluated at the critical point.

To first order this is a linear system of equations that is solved in terms of exponential functions and only a relatively small number of flow patterns are possible. These patterns are determined by the invariants of the velocity gradient tensor *A*.

STANFORD
AERONAUTICS &
ASTRONAUTICS

Linear flows in two dimensions.

The eigenvalues of *A* satisfy.

$$\lambda^2 + P\lambda + Q = 0$$

where.

$$P = -A_{ii} \quad ; \qquad Q = Det(A_{ik}) \, .$$

The solution is.

$$\lambda = -\frac{P}{2} \pm \frac{1}{2}\sqrt{P^2 - 4Q} \, .$$

The topology of the local flow is determined by the sign of the quadratic discriminant.

$$D = Q - \frac{P^2}{4} \, .$$

STANFORD
AERONAUTICS &
ASTRONAUTICS

The various possible flow patterns can be described in a cross-plot of the invariants.

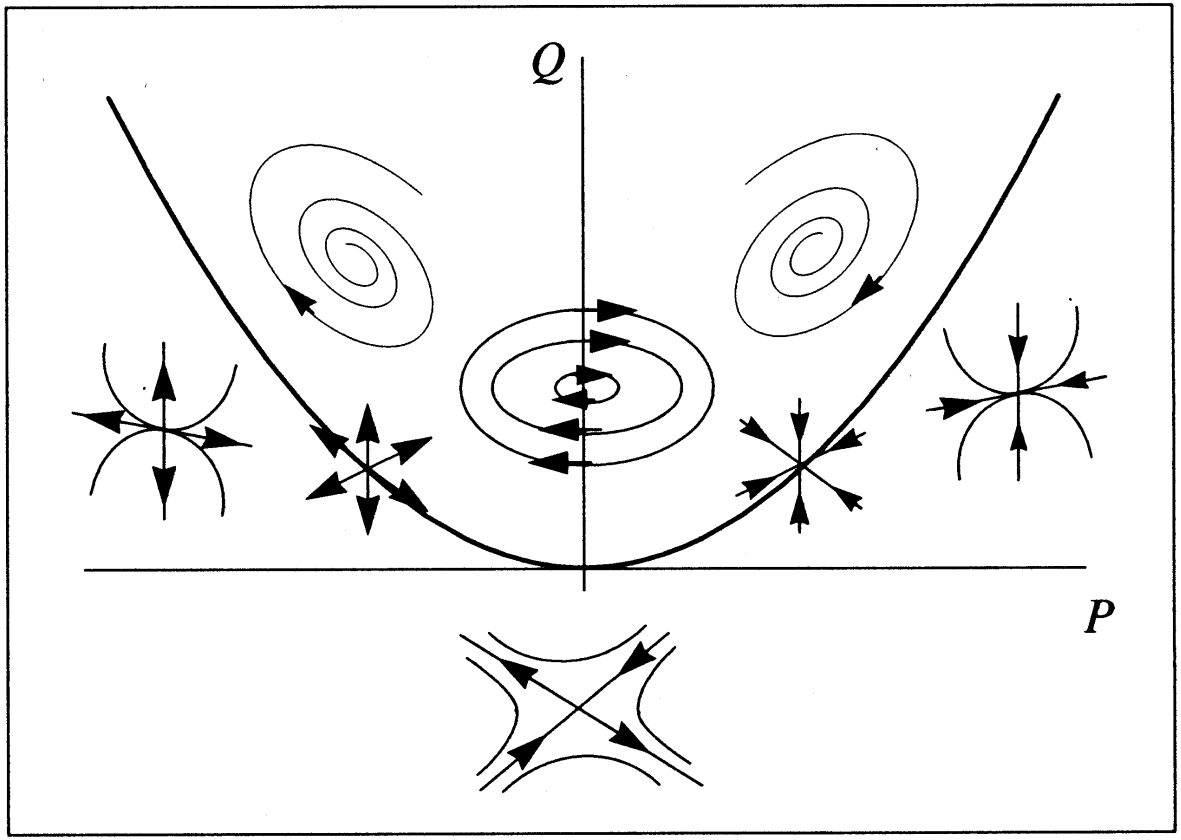

Figure 4.1 Classification of linear flows in two dimensions

STANFORD
AERONAUTICS &
ASTRONAUTICS

2-D Point source in a uniform stream.

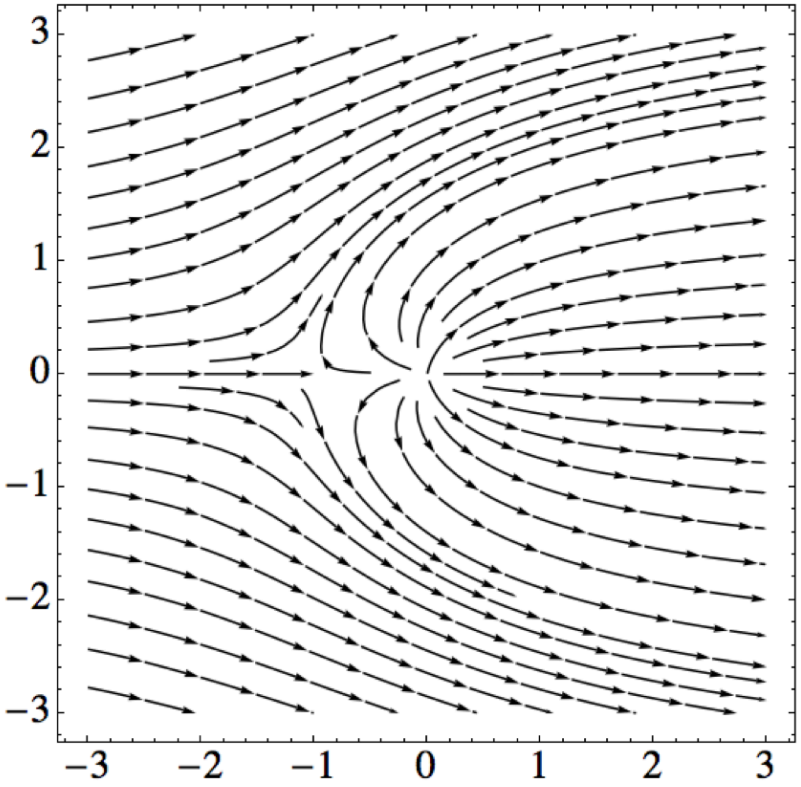

Velocity potential.

$$\Phi = U_\infty x + \frac{\dot{A}}{4\pi} Ln\left(x^2 + y^2\right)$$

STANFORD
AERONAUTICS &
ASTRONAUTICS

Velocity field and derivatives.

$$U = \frac{\partial \Phi}{\partial x} = U_\infty + \frac{\dot{A}}{2\pi}\frac{x}{\left(x^2+y^2\right)}$$

$$V = \frac{\partial \Phi}{\partial y} = \frac{\dot{A}}{2\pi}\frac{y}{\left(x^2+y^2\right)}$$

$$\frac{\partial U}{\partial x} = \frac{\dot{A}}{2\pi}\frac{\left(x^2+y^2\right)-2x^2}{\left(x^2+y^2\right)^2}$$

$$\frac{\partial U}{\partial y} = \frac{\dot{A}}{\pi}\frac{-xy}{\left(x^2+y^2\right)^2}$$

$$\frac{\partial V}{\partial x} = \frac{\dot{A}}{\pi}\frac{-xy}{\left(x^2+y^2\right)}$$

$$\frac{\partial V}{\partial y} = \frac{\dot{A}}{2\pi}\frac{\left(x^2+y^2\right)-2y^2}{\left(x^2+y^2\right)^2}$$

STANFORD
AERONAUTICS &
ASTRONAUTICS

Critical point is at $$(x_c, y_c) = \left(-\frac{\dot{A}}{2\pi U_\infty}, 0 \right)$$

Near the critical point.

$$\begin{bmatrix} U \\ V \end{bmatrix} = \left[\begin{matrix} \frac{\partial U}{\partial x} & \frac{\partial U}{\partial y} \\ \frac{\partial V}{\partial x} & \frac{\partial V}{\partial y} \end{matrix} \right]_{(x,y)=(x_c,y_c)} \begin{bmatrix} x - x_c \\ y - y_c \end{bmatrix}$$

$$\begin{bmatrix} U \\ V \end{bmatrix} = \begin{bmatrix} -\frac{2\pi U_\infty{}^2}{\dot{A}} & 0 \\ 0 & \frac{2\pi U_\infty{}^2}{\dot{A}} \end{bmatrix} \begin{bmatrix} x - x_c \\ y - y_c \end{bmatrix}$$

Invariants.

$$P = 0$$

$$Q = -\frac{4\pi^2 U_\infty{}^4}{\dot{A}^2}$$

Irrotational saddle point.
Eigenvectors are orthogonal

STANFORD
AERONAUTICS &
ASTRONAUTICS

Problem 1.5

$$\frac{dx}{dt} = Cos(x)Cos(y)$$

$$\frac{dy}{dt} = Sin(x)Sin(y)$$

$$\longrightarrow \quad \psi = Cos(x)Sin(y)$$

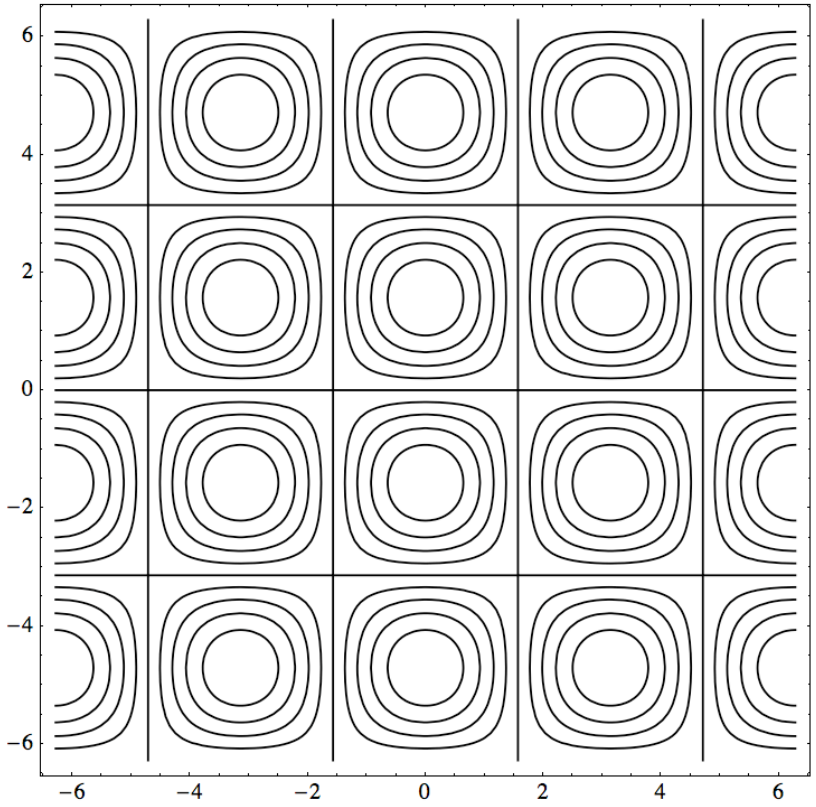

STANFORD
AERONAUTICS &
ASTRONAUTICS

Experiment to measure separated flow

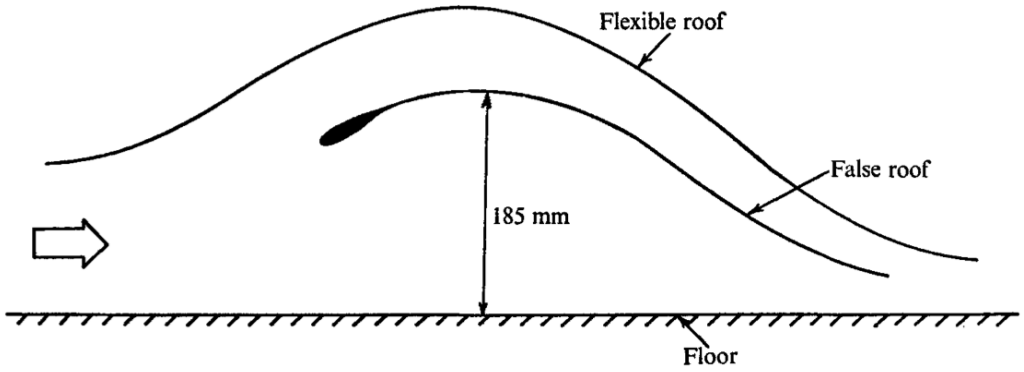

FIGURE 4. Arrangement of false roof. Duct width = 610 mm.

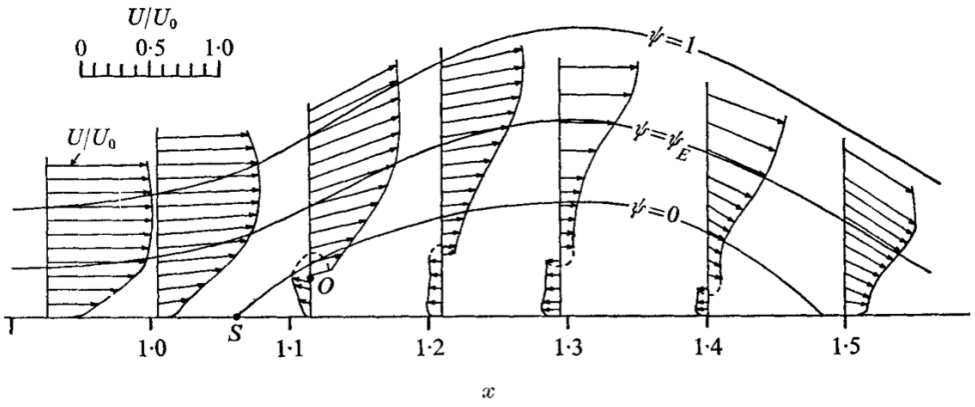

FIGURE 5. Velocity vector field for case 1 obtained from experiment.

Perry and Fairlie - A study of turbulent boundary layer separation and reattachment, *Journal of Fluid Mechanics* Vol 69, 1975

STANFORD
AERONAUTICS &
ASTRONAUTICS

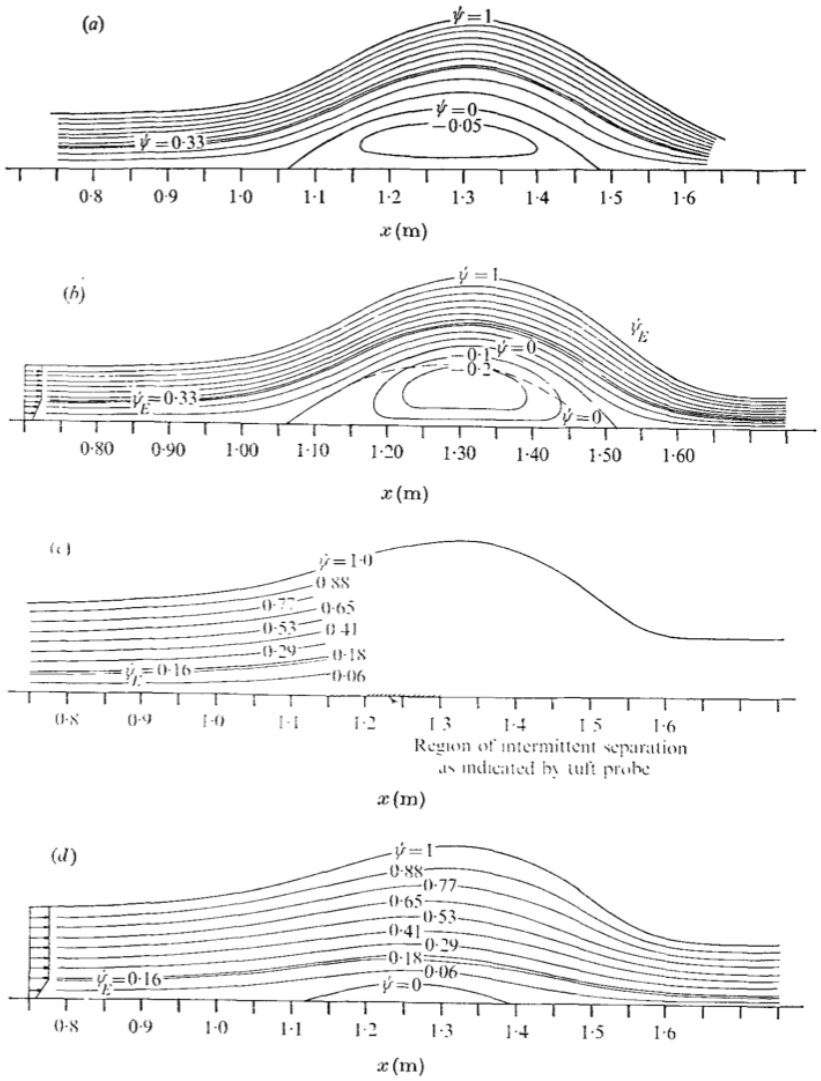

FIGURE 6. Streamline patterns for (*a*) case 1, experiment; (*b*) case 1, analog solution; (*c*) case 2, experiment; (*d*) case 2, analog solution.

Low Re

High Re

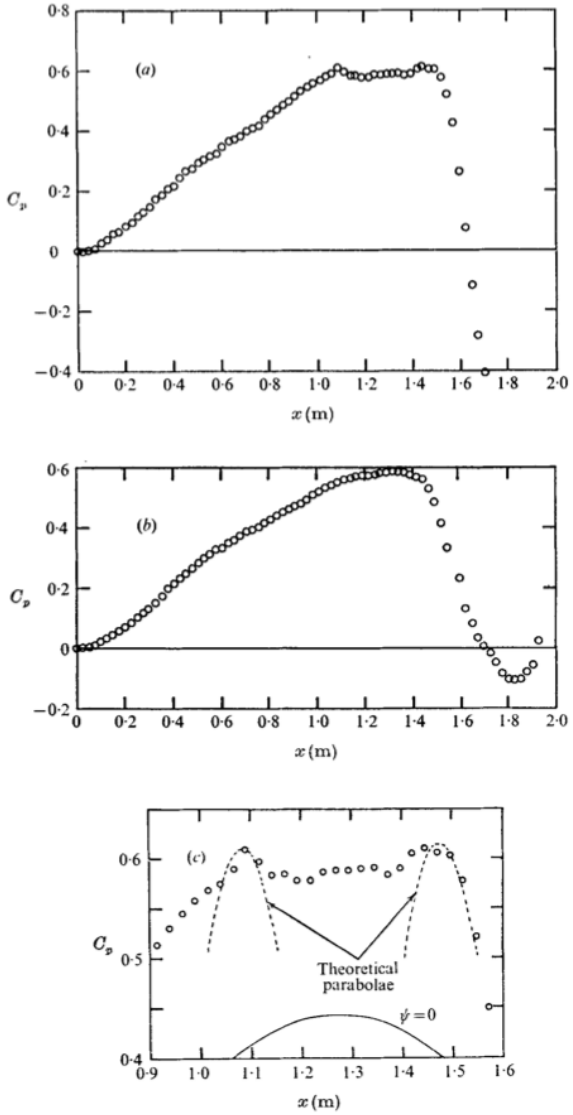

FIGURE 7. Surface pressure distributions. (*a*) Case 1. (*b*) Case 2. (*c*) Detail in separated region of case 1 showing osculating parabolae. $C_p = (P - P_{x=0})/\frac{1}{2}\rho(U_1)^2_{x=0}$. (After Perry & Fairlie 1974.)

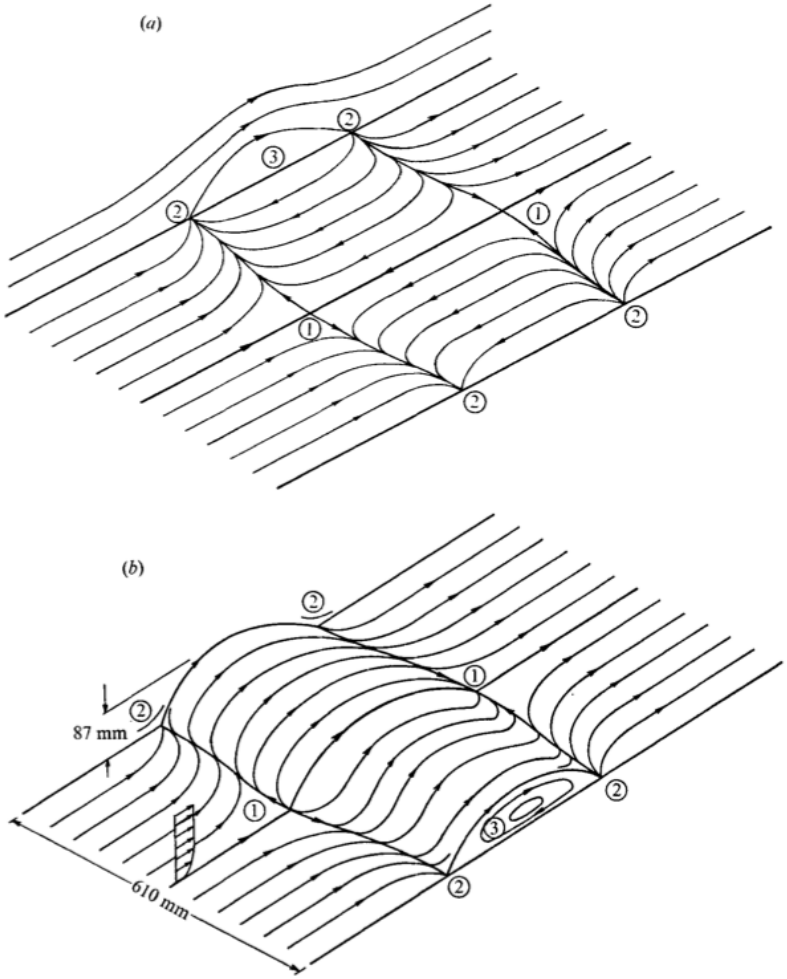

FIGURE 8. Flow patterns for case 1 showing classification of critical points. (*a*) Surface streamlines. (*b*) 'Separation surface' streamlines. 1, 'saddle' in plane of floor, 'node' in plane of separation surface; 2, 'node' in plane of floor, 'saddle' in plane of side wall; 3, 'centre' on side wall.

STANFORD
AERONAUTICS &
ASTRONAUTICS

Linear flows in three dimensions.

The eigenvalues of *A* satisfy a cubic equation.

$$\lambda^3 + P\lambda^2 + Q\lambda + R = 0$$

The invariants P, Q and R are related to powers of *A*.

$$\left.\begin{aligned} P &= -tr[\boldsymbol{A}] = -A_{ii} \\ Q &= \frac{1}{2}(P^2 - tr[\boldsymbol{A}^2]) = \frac{1}{2}(P^2 - A_{ik}A_{ki}) \\ R &= \frac{1}{3}(-P^3 + 3PQ - tr[\boldsymbol{A}^3]) = \frac{1}{3}(-P^3 + 3PQ - A_{ik}A_{km}A_{mi}) \end{aligned}\right\}.$$

Solutions are either all real or one real and two complex conjugates.

The quadratic term can be eliminated by the following change of variables.

$$\lambda = \alpha - \frac{P}{3}$$

$$\alpha^3 + \hat{Q}\alpha + \hat{R} = 0$$

The new invariants are as follows.

$$\hat{Q} = Q - \frac{1}{3}P^2 \quad ; \qquad \hat{R} = R - \frac{1}{3}PQ + \frac{2}{27}P^3$$

STANFORD
AERONAUTICS &
ASTRONAUTICS

The solution of the modified cubic is generated as follows. Let

$$a_1 = \left(-\frac{\hat{R}}{2} + \frac{1}{3\sqrt{3}} \left(\hat{Q}^3 + \frac{27}{4}\hat{R}^2 \right)^{\frac{1}{2}} \right)^{\frac{1}{3}}; \quad a_2 = \left(-\frac{\hat{R}}{2} - \frac{1}{3\sqrt{3}} \left(\hat{Q}^3 + \frac{27}{4}\hat{R}^2 \right)^{\frac{1}{2}} \right)^{\frac{1}{3}}$$

The real solution is

$$\alpha_1 = a_1 + a_2$$

and the complex or remaining real solutions are

$$\alpha_2 = -\frac{1}{2}(a_1 + a_2) + \frac{i\sqrt{3}}{2}(a_1 - a_2)$$

$$\alpha_3 = -\frac{1}{2}(a_1 + a_2) - \frac{i\sqrt{3}}{2}(a_1 - a_2)$$

When solving a cubic equation one is led to the cubic discriminant.

$$D = \frac{27}{4}R^2 + \left(P^3 - \frac{9}{2}PQ\right)R + Q^2\left(Q - \frac{1}{4}P^2\right).$$

The surface D=0 is shown below.

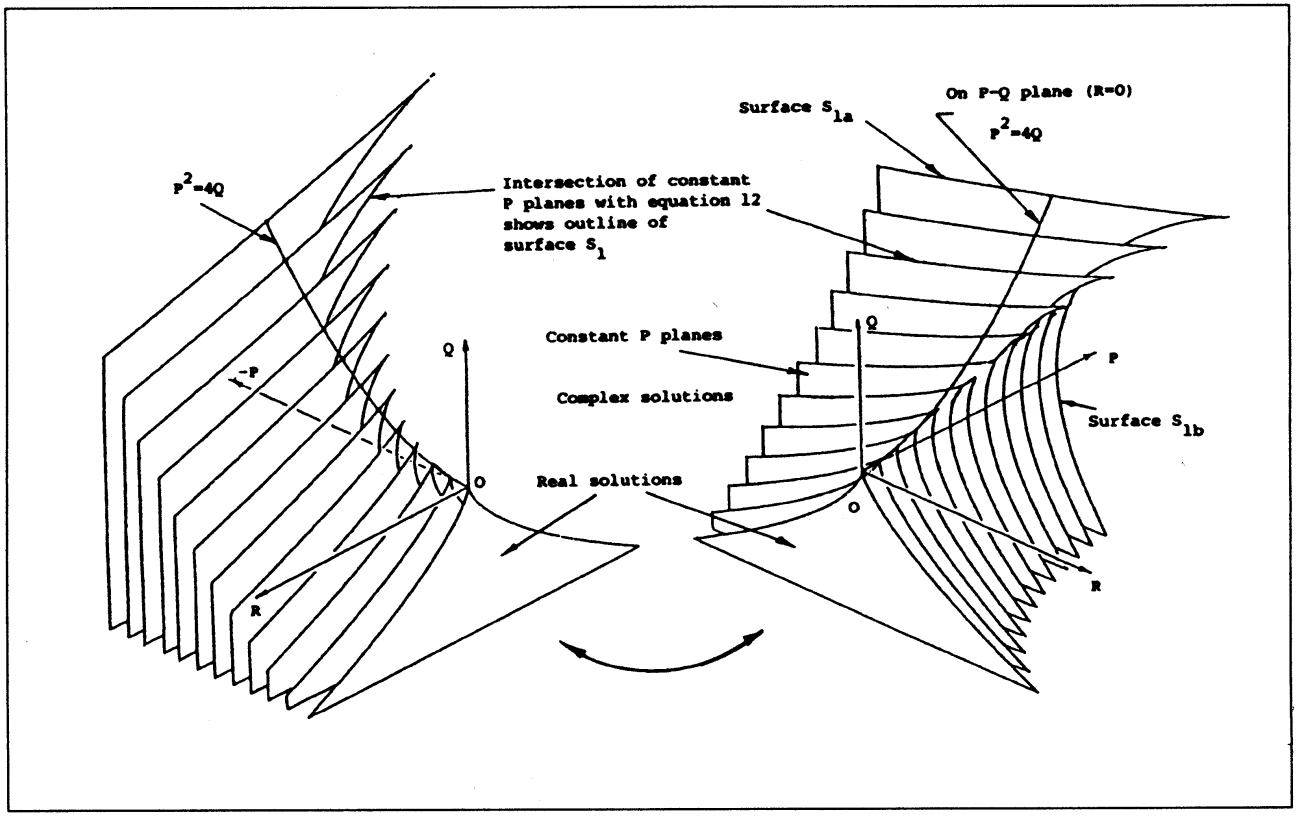

If the eigenvalues are all real then the invariants can be expressed as follows.

$$\left.\begin{aligned} P &= -(\lambda^1 + \lambda^2 + \lambda^3) \\ Q &= \lambda^1\lambda^2 + \lambda^1\lambda^3 + \lambda^2\lambda^3 \\ R &= -\lambda^1\lambda^2\lambda^3 \end{aligned}\right\}$$

If the eigenvalues are one real and two complex conjugate then the invariants can be expressed as follows.

$$\left.\begin{aligned} P &= -(2\sigma + b) \\ Q &= \sigma^2 + \omega^2 + 2\sigma b \\ R &= -b(\sigma^2 + \omega^2) \end{aligned}\right\}$$

Where *b* is the real eigenvalue and sigma and omega are the real and imaginary parts of the complex conjugate eigenvalues.

Three-dimensional incompressible flow patterns are characterized by

$$\nabla \bullet U = \frac{\partial U_i}{\partial x_i} = A_{ii} = 0.$$

This corresponds to *P=0*.

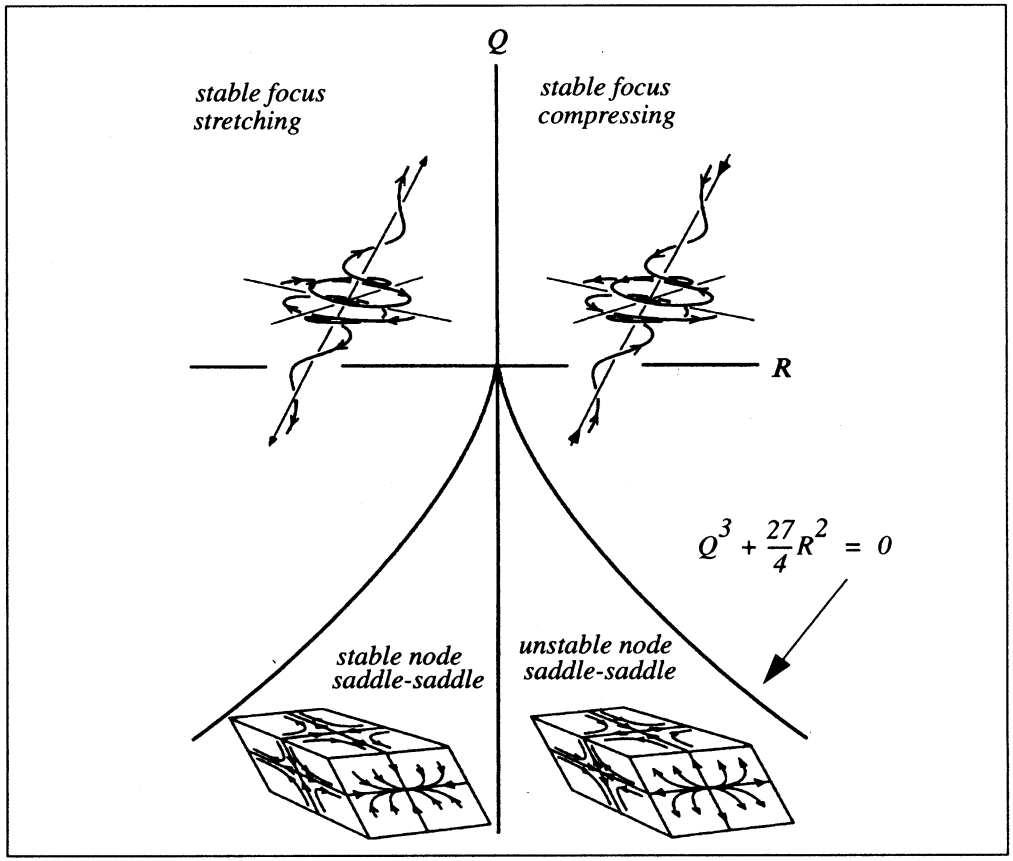

In this case the cubic discriminant simplifies to

$$D = Q^3 + \frac{27}{4}R^2$$

and the invariants are

$$Q = -\frac{1}{2}A_{ik}A_{ki} \quad , \qquad R = -\frac{1}{3}A_{ik}A_{km}A_{mi} \; .$$

STANFORD
AERONAUTICS &
ASTRONAUTICS

Frames of reference.

For a general smooth flow the particle path equations can be expanded in a Taylor series about any point x_0.

$$\frac{dx_i}{dt} = U_i\Big|_{\bar{x}=\bar{x}_0} + A_{ik}\Big|_{\bar{x}=\bar{x}_0}(x_k - x_{0k}) + O((x_k - x_{0k})^2) + \ldots.$$

Transform to a frame of reference attached to and moving with a fluid element at the point x_0. The position and velocity in the moving coordinates are

$$\bar{x}' = \bar{x} - \bar{x}_0$$

$$\bar{U}' = \bar{U} - \bar{U}\Big|_{\bar{x}=\bar{x}_0}$$

The flow pattern seen by the moving observer is determined by

$$\frac{dx'_i}{dt} = A_{ik}\Big|_{\bar{x}'=0} x'_k + O(x'^2_k) + \ldots$$

The velocity gradient tensor determines the local flow pattern seen in a frame of reference moving with a fluid element.

STANFORD
AERONAUTICS &
ASTRONAUTICS

4.2 Rate-of-strain and Rate-of-rotation tensors

The velocity gradient tensor.

$$A_{ij} = \partial U_i / \partial x_j .$$

Can be split into a symmetric and an anti-symmetric part.

$$A_{ij} = \frac{\partial U_i}{\partial x_j} = \frac{1}{2}\left(\frac{\partial U_i}{\partial x_j} + \frac{\partial U_j}{\partial x_i}\right) + \frac{1}{2}\left(\frac{\partial U_i}{\partial x_j} - \frac{\partial U_j}{\partial x_i}\right).$$

The symmetric part is the rate-of-strain tensor.

$$S_{ij} = \frac{1}{2}\left(\frac{\partial U_i}{\partial x_j} + \frac{\partial U_j}{\partial x_i}\right)$$

The anti-symmetric part is the rate-of-rotation or spin tensor.

$$W_{ij} = \frac{1}{2}\left(\frac{\partial U_i}{\partial x_j} - \frac{\partial U_j}{\partial x_i}\right).$$

The vorticity vector is related to the spin tensor.

$$\Omega_i = \varepsilon_{ijk}(\partial U_k / \partial x_j)$$

$$W_{ik} = \frac{1}{2}\varepsilon_{ijk}\Omega_j .$$

STANFORD
AERONAUTICS &
ASTRONAUTICS

Viscous incompressible Flow near a wall

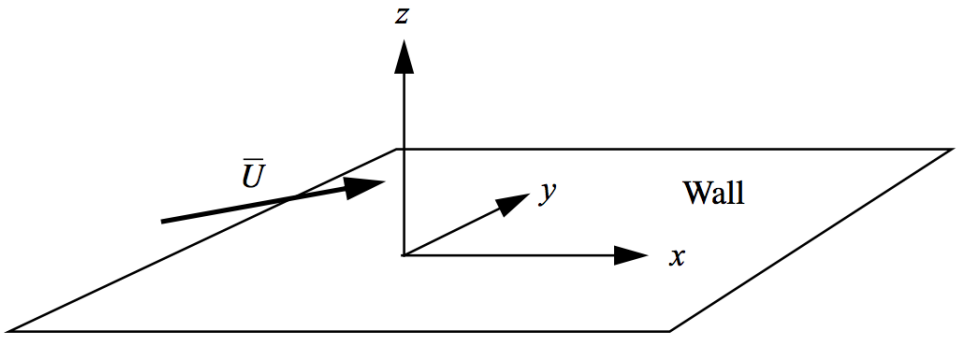

Expand the velocity field near the wall up to second order.

$$U = A_{11}x + A_{12}y + A_{13}z + B_{111}x^2 + B_{112}xy + B_{113}xz + B_{122}y^2 + B_{123}yz + B_{133}z^2 \quad (5.35)$$

$$V = A_{21}x + A_{22}y + A_{23}z + B_{211}x^2 + B_{212}xy + B_{213}xz + B_{222}y^2 + B_{223}yz + B_{233}z^2$$

$$W = A_{31}x + A_{32}y + A_{33}z + B_{311}x^2 + B_{312}xy + B_{313}xz + B_{322}y^2 + B_{323}yz + B_{333}z^2$$

Derivatives of the velocity in the (x,y) plane are zero to all orders. Therefore

$$\begin{aligned} A_{11} &= A_{12} = B_{111} = B_{112} = B_{122} = 0 \\ A_{21} &= A_{22} = B_{211} = B_{212} = B_{222} = 0 \\ A_{31} &= A_{32} = B_{311} = B_{312} = B_{322} = 0 \end{aligned} \quad (5.36)$$

The velocity field near the wall reduces to

$$\begin{aligned} U &= A_{13}z + B_{113}xz + B_{123}yz + B_{133}z^2 \\ V &= A_{23}z + B_{213}xz + B_{223}yz + B_{233}z^2 \\ W &= A_{33}z + B_{313}xz + B_{323}yz + B_{333}z^2 \end{aligned} \tag{5.37}$$

Apply the continuity equation.

$$\frac{\partial U}{\partial x} + \frac{\partial V}{\partial y} + \frac{\partial W}{\partial z} = A_{33} + (B_{113} + B_{223} + 2B_{333})z + B_{313}x + B_{323}y = 0 \tag{5.38}$$

The coordinates x, y, z are arbitrary so continuity is satisfied only if.

$$\begin{aligned} A_{33} &= 0 \\ B_{113} + B_{223} + 2B_{333} &= 0 \\ B_{313} &= B_{323} = 0 \end{aligned} \tag{5.39}$$

The viscous incompressible stress tensor also simplifies

$$\left.\frac{\tau_{ij}}{\rho}\right|_{z=0} = \nu \begin{pmatrix} 2\frac{\partial U}{\partial x} & \left(\frac{\partial U}{\partial y}+\frac{\partial V}{\partial x}\right) & \left(\frac{\partial U}{\partial z}+\frac{\partial W}{\partial x}\right) \\ \left(\frac{\partial U}{\partial y}+\frac{\partial V}{\partial x}\right) & 2\frac{\partial V}{\partial y} & \left(\frac{\partial V}{\partial z}+\frac{\partial W}{\partial y}\right) \\ \left(\frac{\partial U}{\partial z}+\frac{\partial W}{\partial x}\right) & \left(\frac{\partial V}{\partial z}+\frac{\partial W}{\partial y}\right) & 2\left(\frac{\partial W}{\partial z}\right) \end{pmatrix}_{z=0} = \nu \begin{pmatrix} 0 & 0 & \left(\frac{\partial U}{\partial z}\right) \\ 0 & 0 & \left(\frac{\partial V}{\partial z}\right) \\ \left(\frac{\partial U}{\partial z}\right) & \left(\frac{\partial V}{\partial z}\right) & 0 \end{pmatrix}_{z=0} \tag{5.40}$$

The surface traction vector reduces to a two-dimensional vector field in the wall

$$F_{i_{wall}} = \left.\frac{\tau_{ij}}{\rho} n_j\right|_{z=0} = \nu \begin{bmatrix} 0 & 0 & \frac{\partial U}{\partial z} \\ 0 & 0 & \frac{\partial V}{\partial z} \\ \frac{\partial U}{\partial z} & \frac{\partial V}{\partial z} & 0 \end{bmatrix} \begin{bmatrix} 0 \\ 0 \\ n_z \end{bmatrix} = \nu \begin{bmatrix} \frac{\partial U}{\partial z} n_z \\ \frac{\partial V}{\partial z} n_z \\ 0 \end{bmatrix} = \begin{bmatrix} F_x \\ F_y \\ 0 \end{bmatrix} \tag{5.41}$$

n_z is a unit vector normal to the wall $\quad \left.\frac{\partial U}{\partial z}\right|_{z=0} = A_{13} \qquad \left.\frac{\partial V}{\partial z}\right|_{z=0} = A_{23}$

STANFORD
AERONAUTICS &
ASTRONAUTICS

Scale the velocity field by the distance from the wall.

$$\frac{U}{z} = \frac{F_x}{\nu} + B_{113}x + B_{123}y + B_{133}z$$

$$\frac{V}{z} = \frac{F_y}{\nu} + B_{213}x + B_{223}y + B_{233}z \qquad (5.42)$$

$$\frac{W}{z} = -\frac{(B_{113} + B_{223})}{2}z$$

The wall viscous traction vector can be viewed as defining limiting streamlines at the surface.

Critical points occur where $\left(F_x, F_y\right) = (0,0)$

Three-dimensional "No-slip" critical points are characterized using

$$\frac{dx}{d\tau} = B_{113}x + B_{123}y + B_{133}z$$

$$\frac{dy}{d\tau} = B_{213}x + B_{223}y + B_{233}z \qquad (5.43)$$

$$\frac{dz}{d\tau} = -\frac{(B_{113} + B_{223})}{2}z$$

where

$$d\tau = z\,dt$$

is a scaled time

STANFORD
AERONAUTICS &
ASTRONAUTICS

Model of a three-dimensional separation bubble.

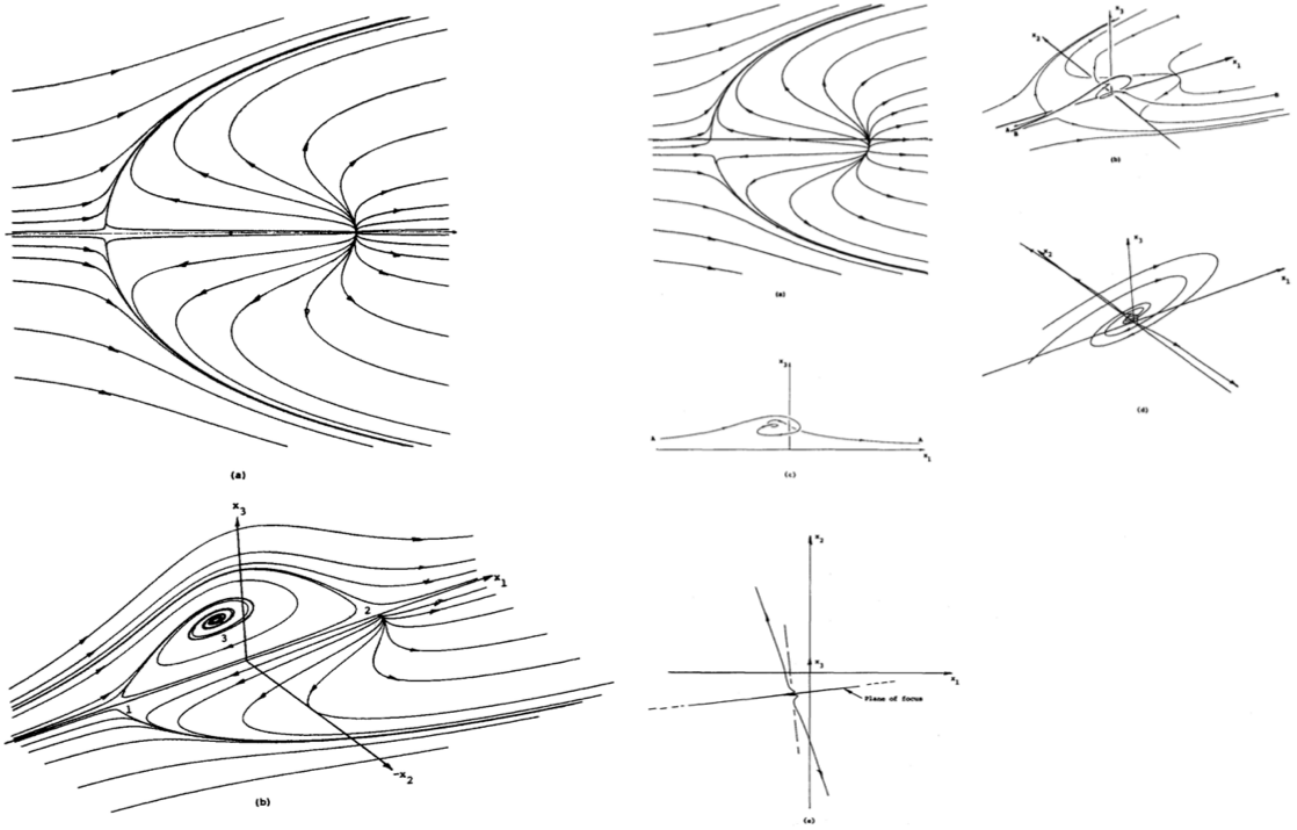

Figure 5.5 Model flow used to study three-dimensional separation. On the left limiting streamlines at the wall are shown with streamlines in a symmetry plane normal to the wall. On the lft a small degree of asymmetry is added to the flow along with depiction of several individual streamlines.

STANFORD
AERONAUTICS &
ASTRONAUTICS

Traction vector lines on a sphere. $\sum N - \sum S = 2$

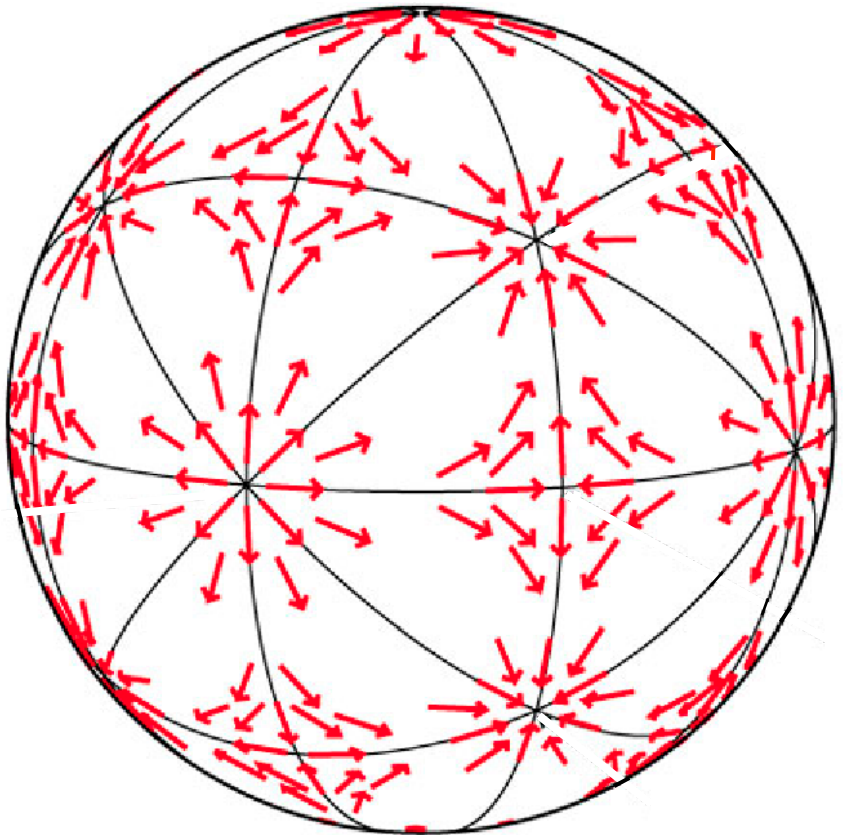

The "hairy tennis ball" theorem

STANFORD
AERONAUTICS &
ASTRONAUTICS

Topological rules

1. Skin-friction lines on a three-dimensional body (Davey 1961, Lighthill 1963):

$$\sum_N - \sum_S = 2 . \tag{6}$$

2. Skin-friction lines on a three-dimensional body B connected simply (without gaps) to a plane wall P that either extends to infinity both upstream and downstream or is the surface of a torus:

$$\left(\sum_N - \sum_S \right)_{P+B} = 0 . \tag{7}$$

3. Streamlines on a two-dimensional plane cutting a three-dimensional body:

$$\left(\sum_N + \frac{1}{2} \sum_{N'} \right) - \left(\sum_S + \frac{1}{2} \sum_{S'} \right) = -1 . \tag{8}$$

4. Streamlines on a vertical plane cutting a surface that extends to infinity both upstream and downstream:

$$\left(\sum_N + \frac{1}{2} \sum_{N'} \right) - \left(\sum_S + \frac{1}{2} \sum_{S'} \right) = 0 . \tag{9}$$

5. Streamlines on the projection onto a spherical surface of a conical flow past a three-dimensional body (Smith 1969):

$$\left(\sum_N + \frac{1}{2} \sum_{N'} \right) - \left(\sum_S + \frac{1}{2} \sum_{S'} \right) = 0 . \tag{10}$$

Murray Tobak and David Peake - Topology of three-dimensional separated flows *Annual Reviews of Fluid Mechanics* 1982

Oil flow, china clay visualization

These ideas form the basis of a method for visualizing the flow near a wall using drops of pigmented oil placed on the surface of a body.

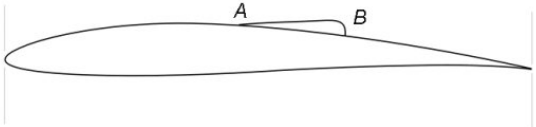

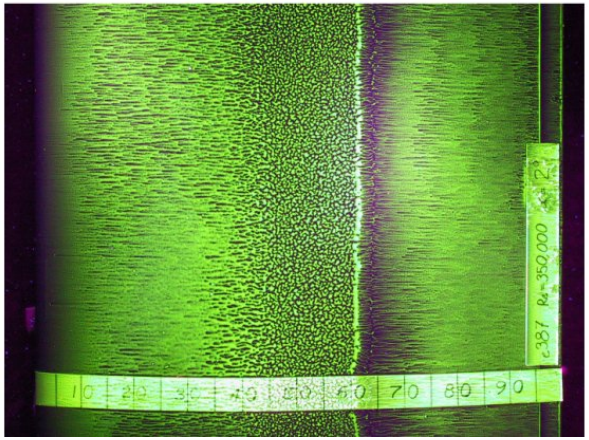

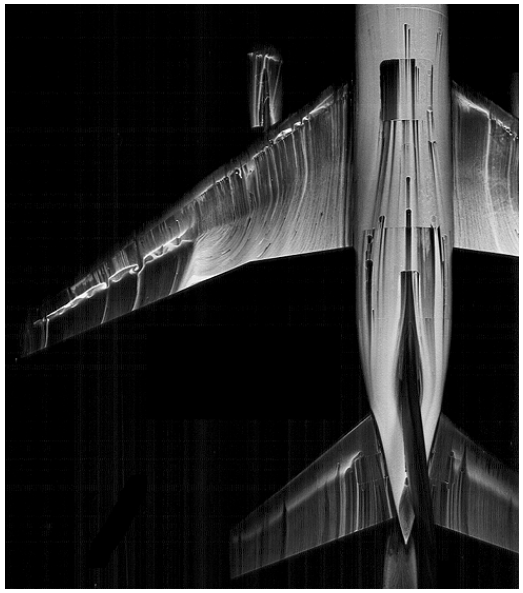

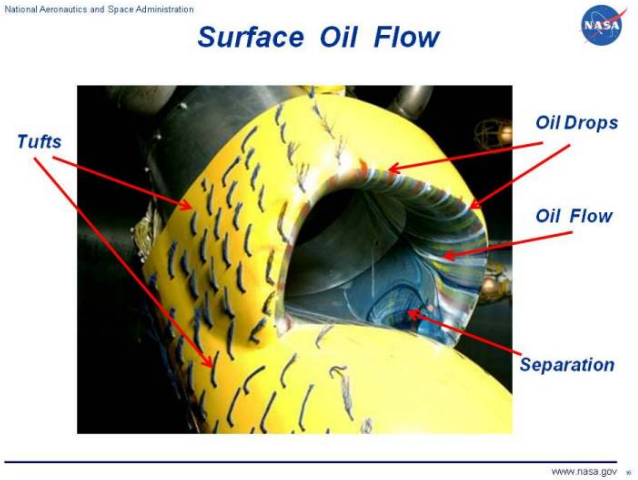

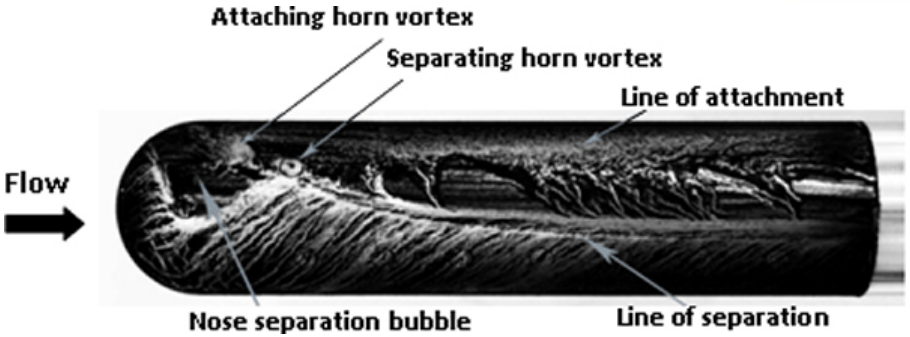

STANFORD
AERONAUTICS &
ASTRONAUTICS

3-D Separation

Topological methods have greatly improved our understanding of 3-D separated flows.

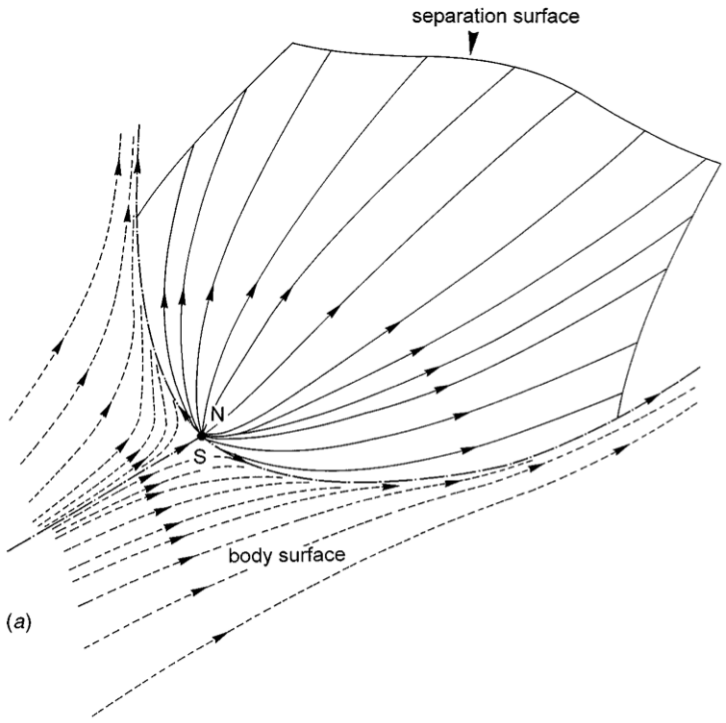

Figure 6 Flow behavior in the vicinity of a separator line: (*a*) separation process, (*b*) attachment process.

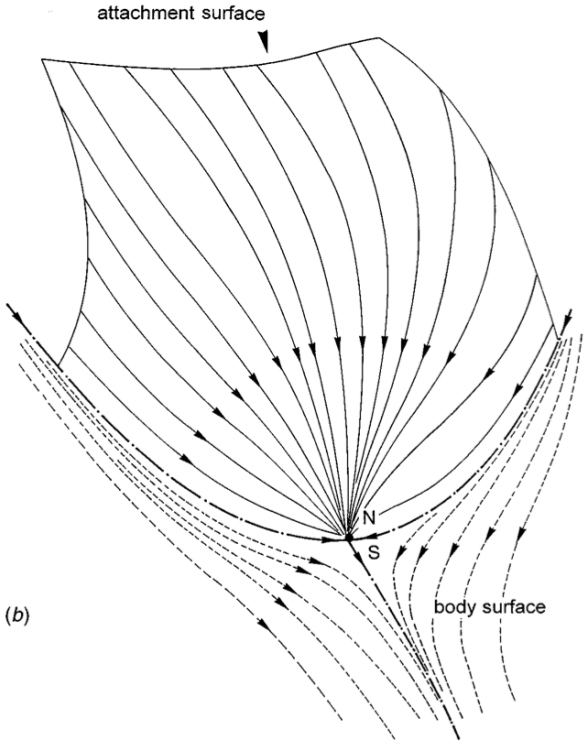

Figure 6 (*continued*)

Jean Delery - Robert Legendre and Henri Werle: Toward the elucidation of three-dimensional separation *Annual Reviews of Fluid Mechanics* 33, 2001

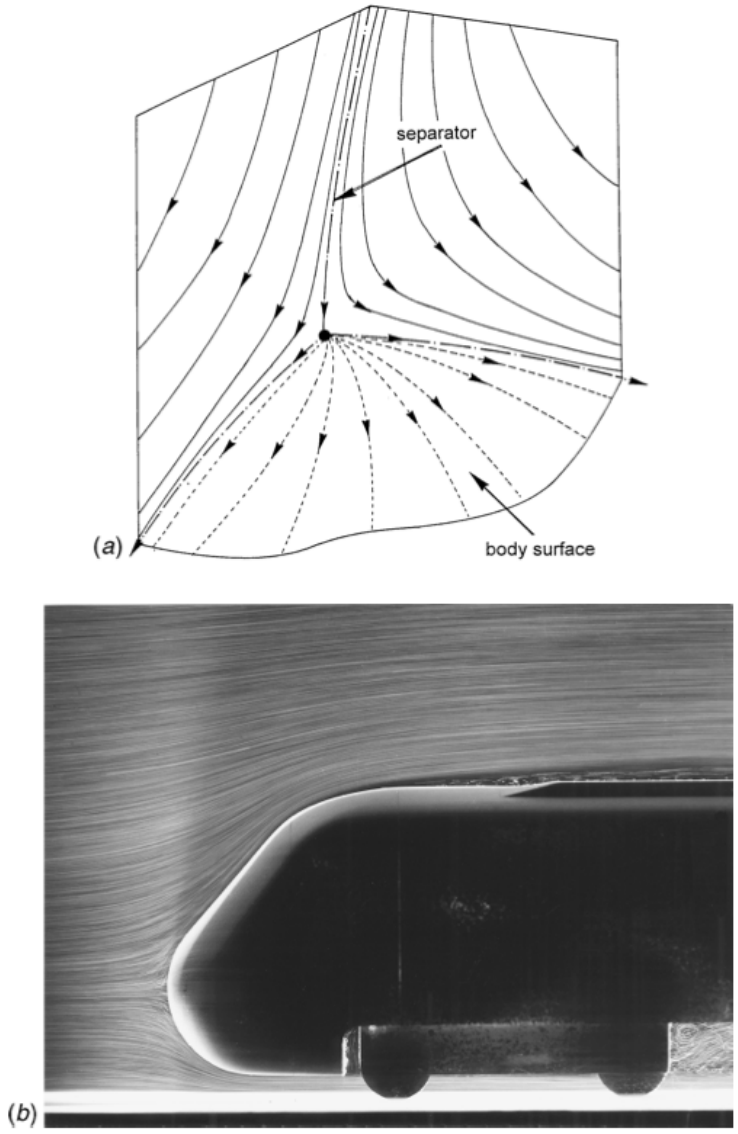

Figure 7 Three-dimensional saddle point: (*a*) sketch of the flow field topology, (*b*) attachment point on a high-speed train.

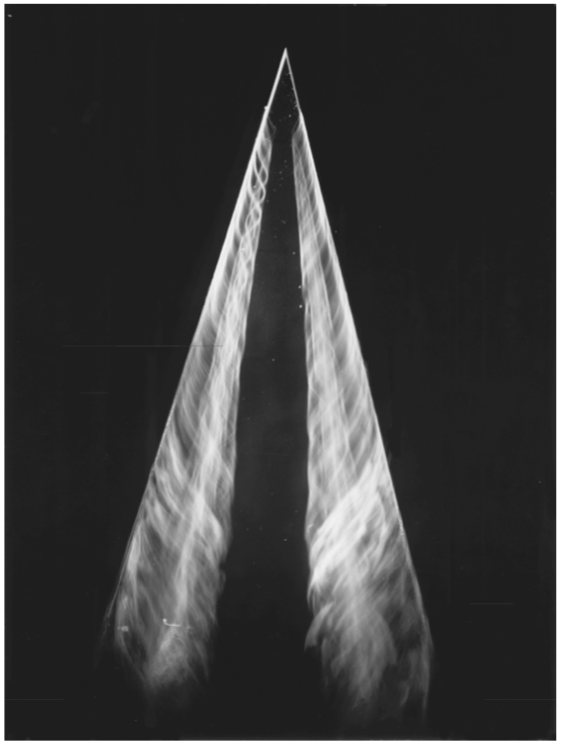

Figure 9 Vortices over a 75°-sweep angle delta wing.

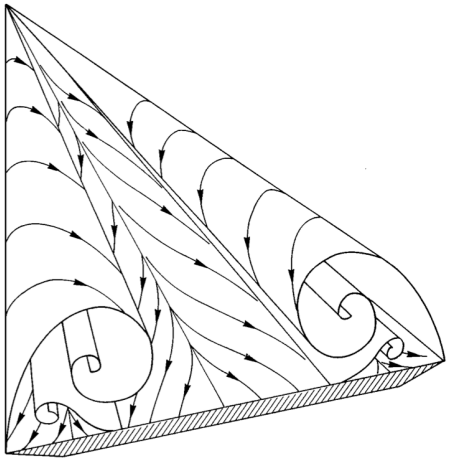

Figure 14 Schematic representation of the separation surfaces over a highly swept delta wing.

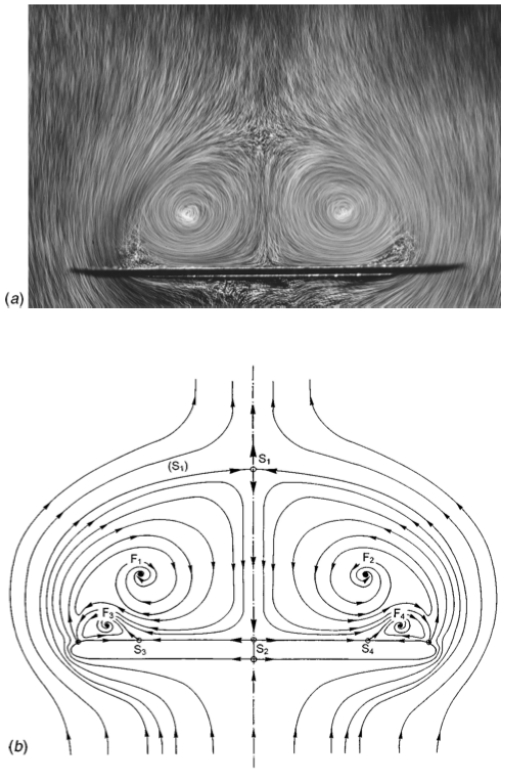

Figure 10 Cross flow over a 75°-sweep angle delta wing: (*a*) air bubbles visualization, (*b*) topological interpretation.

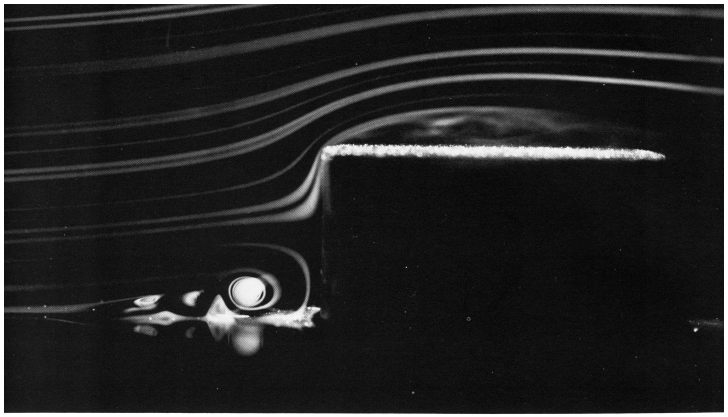

92. Horseshoe vortices ahead of a cylinder in a boundary layer. The laminar boundary layer on a flat plate separates ahead of a short circular cylinder, whose height is about three times the boundary-layer thickness. The vorticity in the boundary layer concentrates into three vortices that wrap around the front of the cylinder. Closer to the plate, two vortices of opposite sign form in the reverse flow, and are reflected in the plate. The Reynolds number is 5000 based on cylinder diameter. Visualization is by smoke filaments in air, illuminated by a thin slice of light in the symmetry plane. This shows three stagnation points on the plate, three points of attachment, and two free stagnation points between the vortices. Another picture of the same flow appears as the frontispiece to Thwaites' *Incompressible Aerodynamics. Photograph from E. P. Sutton and the Cambridge University Engineering Department.*

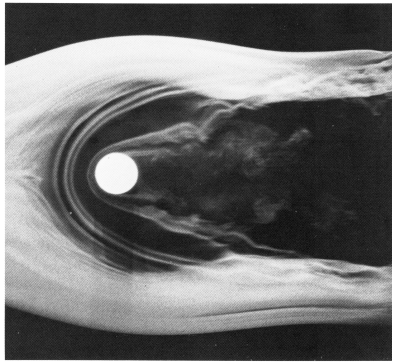

93. Horseshoe vortices ahead of a cylinder in a boundary layer. In this plan view the thickness of the oncoming Blasius boundary layer is one-third of the diameter of the cylinder, as in the photograph above, and the Reynolds number is 4000 based on the diameter, but the cylinder is two diameters rather than half a diameter high. The horseshoe vortices are made visible by a sheet of smoke introduced into the boundary layer upstream. *Photograph by Sadatoshi Taneda*

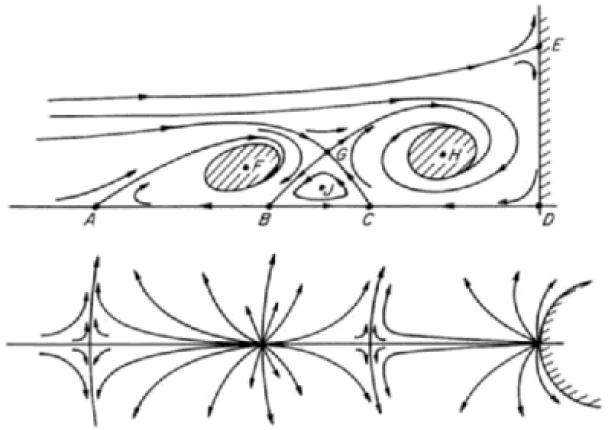

FIG. 9. Laminar separation in front of cylindrical obstruction. *A*, *B*, *C*, *D*, and *E* are viscous critical points. *F*, *G*, *H*, and *J* are inviscid-constant-vorticity critical points. Plan view shows surface trajectories. Note the sequence of saddles and nodes.

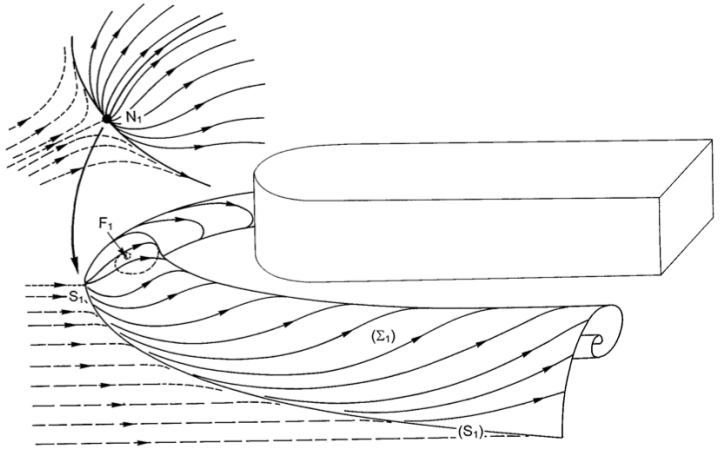

Figure 22 Schematic representation of the horseshoe vortex induced by the obstacle.

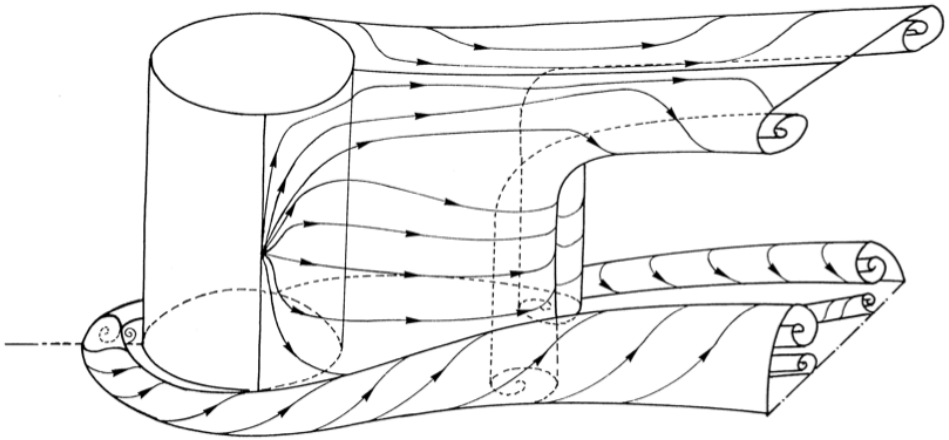

Figure 25 Schematic representation of the vortex system induced by the obstacle.

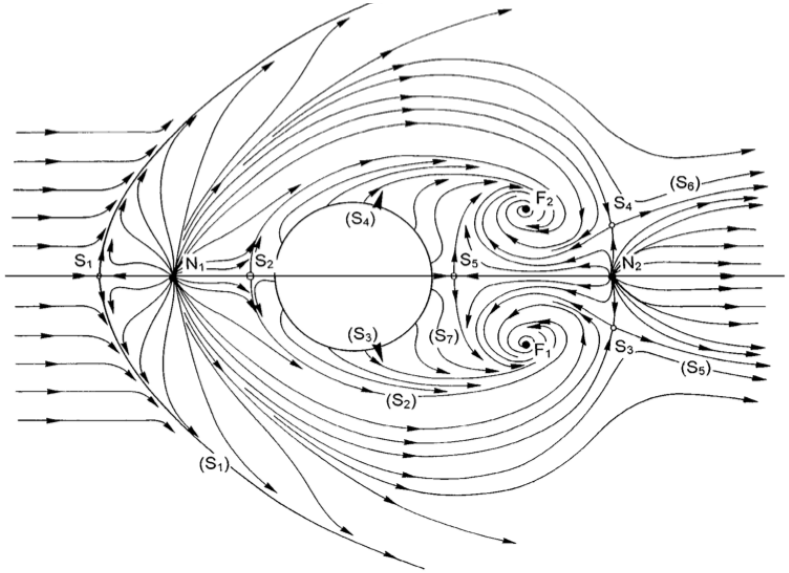

Figure 24 Separation behind a cylindrical obstacle. Topology of the skin-friction-line pattern.

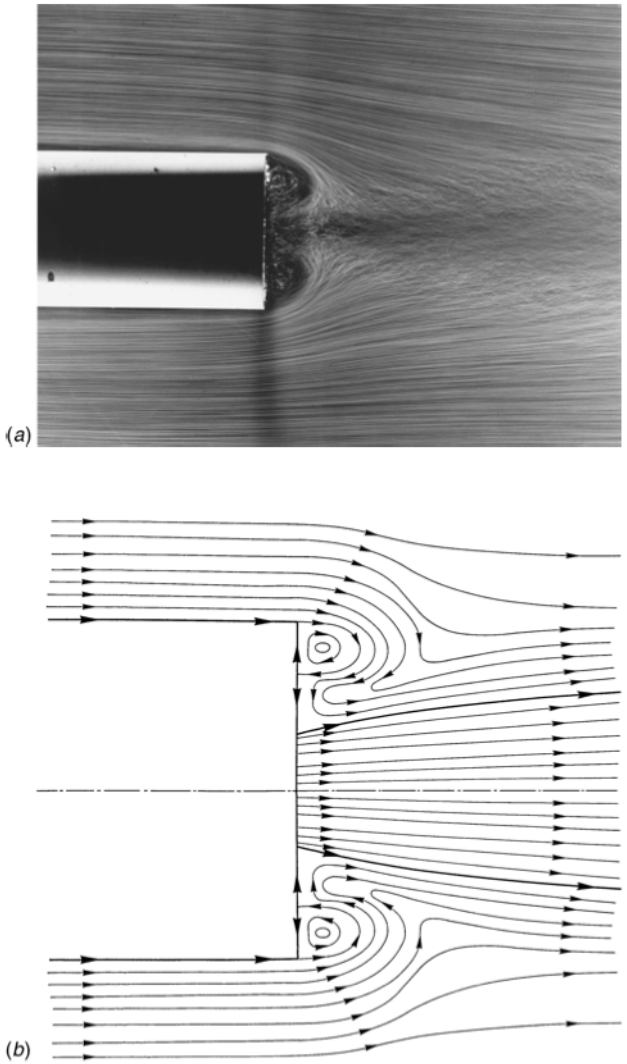

Figure 27 Flow downstream of a cylindrical afterbody with central jet: (*a*) air-bubbles visualization, (*b*) topological interpretation for an axisymmetric field.

STANFORD
AERONAUTICS &
ASTRONAUTICS

A success story

Circa 1985 there was a problem with 3-D separation over the wing upper surface behind the engine nacelle on a Boeing 767 during high angle-of-attack operation. This problem led to a significant loss of lift and poor low speed performance. The problem was studied using oil flow and china clay visualization.

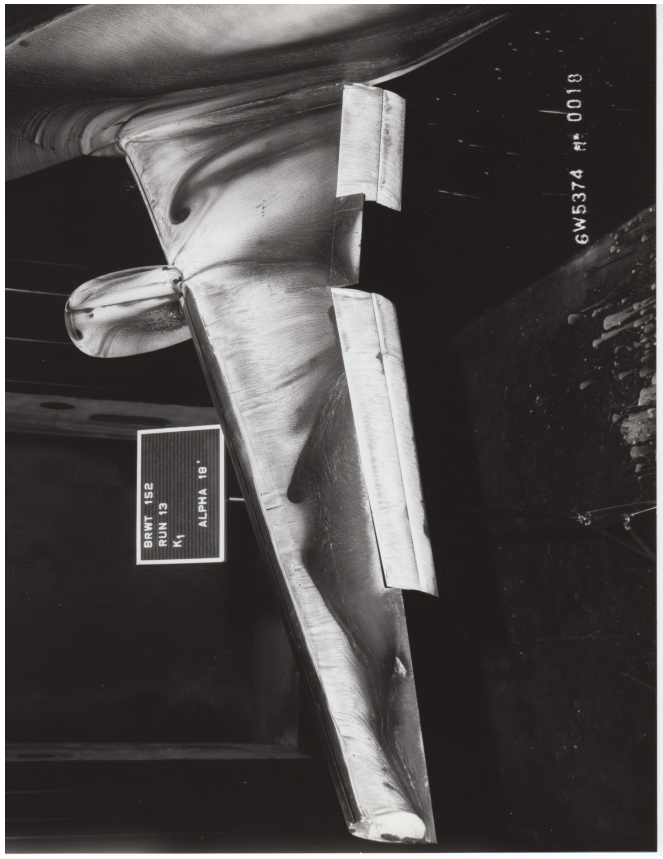

STANFORD
AERONAUTICS &
ASTRONAUTICS

It was decided to add a large vortex generator to the inboard side of the engine nacelle to control the separation. The chine vortex reattaches the flow over the wing and recovers the lost lift during low-speed high angle-of-attack flight. The device reduced approach speeds by 5 knots and landing field length by 250 feet.

STANFORD
AERONAUTICS &
ASTRONAUTICS

Homework Problem

Problem - The image below by Werle shows a visualization of the flow around a circular cylinder attached to a wall in a water channel. The flow is visualized using dye of several colors introduced very close to the wall. This experiment models the effect of tall buildings on the spread of ground contaminants in cities. The atmospheric boundary layer in which the buildings are embedded is on the order of the building height.

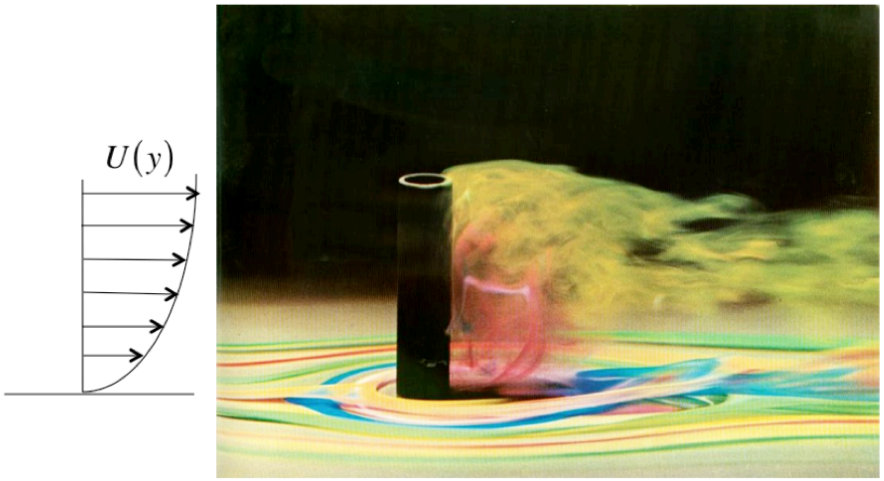

Use reasonable assumptions to determine the dependence of pressure on height along the back of the cylinder. Can you explain the mechanism by which dye is drawn upward from the wall in the near wake of the cylinder?

STANFORD
AERONAUTICS &
ASTRONAUTICS

4.3 Problems

Problem 1 - The simplest 2-D flows imaginable are given by the linear system

$$\frac{dx}{dt} = ax + by$$
$$\frac{dy}{dt} = cx + dy \qquad (4.35)$$

Sketch the corresponding flow pattern for the following cases

i) $(a, b, c, d) = (1, -1, -1, -1)$

ii) $(a, b, c, d) = (1, -3, 1, -1)$

iii) $(a, b, c, d) = (-1, 0, 0, -1)$

Work out the invariants of the velocity gradient tensor as well as the various components of the rate-of-rotation and rate-of-strain tensors and the vorticity vector. Which flows are incompressible?

STANFORD
AERONAUTICS &
ASTRONAUTICS

Problem 2 - An unforced damped pendulum is governed by the second order ODE

$$\frac{d^2\theta}{dt^2} + \beta\frac{d\theta}{dt} + \frac{g}{L}Sin(\theta) = 0 \tag{4.36}$$

Let $x = \theta(t)$ and $y = d\theta/dt$. Use these variables to convert the equation to the canonical form.

$$\begin{aligned} \frac{dx}{dt} &= U(x, y) \\ \frac{dy}{dt} &= V(x, y) \end{aligned} \tag{4.37}$$

Sketch the "streamlines" defined by (4.37). Locate and categorize any critical points according methods developed in this chapter. Identify which points are dominated by rotation and which are dominated by the rate-of-strain. You can do this graphically by drawing line segments of the appropriate slope in (x, y) coordinates. The picture of the flow that results is called the *phase portrait* of the flow in reference to the fact that, for the pendulum, a point in the phase portrait represents the instantaneous relation between the position and velocity of the pendulum. For what value of β can the "flow" defined by the phase portrait be used as a model of an incompressible fluid flow?

STANFORD
AERONAUTICS &
ASTRONAUTICS

Problem 3 - Use (4.14) to reduce (4.12) to (4.15).

Problem 4 - Sketch the flow pattern generated by the 3-D linear system

$$\begin{aligned} \frac{dx}{dt} &= -y \\ \frac{dy}{dt} &= x \\ \frac{dz}{dt} &= z \end{aligned} \tag{4.38}$$

Work out the invariants of the velocity gradient tensor as well as the components of the rate-of-rotation and rate-of-strain tensors and vorticity vector. The vector field plotted in three dimensions is called the *phase space* of the system of ODEs.

In fluid mechanics the phase portrait or phase space is the physical space of the flow.

Problem 5 - Show that

$$S_{ij}A_{ji} = S_{ij}S_{ji} \tag{5.54}$$

and is therefore greater than or equal to zero.

Problem 6 - Work out the formulas for the components of the vorticity vector and show that the spin tensor is related to the vorticity vector by

$$W_{ik} = \frac{1}{2}\varepsilon_{ijk}\Omega_j . \tag{5.55}$$

Problem 7 - The velocity field given below has been used in the fluid mechanics literature to model a two dimensional separation bubble.

$$\begin{aligned} U(x, y) &= -y + 3y^2 + 3x^2y - (2/3)y^3 \\ V(x, y) &= -3xy^2 \end{aligned} \quad . \tag{5.56}$$

Draw the phase portrait and identify critical points.

STANFORD
AERONAUTICS &
ASTRONAUTICS

Problem 8 - Consider the laminar flow near a 2-D separation point.

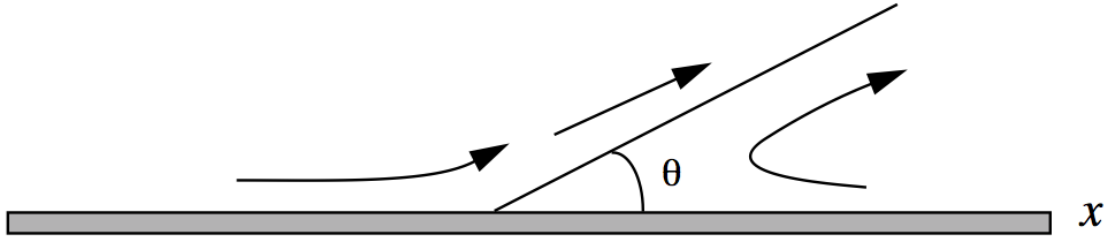

Use an expansion of the velocity field near the wall of the form

$$\begin{aligned} U &= a_{11}x + a_{12}y + b_{111}x^2 + b_{112}xy + b_{122}y^2 \\ V &= a_{21}x + a_{22}y + b_{211}x^2 + b_{212}xy + b_{222}y^2 \end{aligned} \quad . \tag{5.42}$$

Use the 2-D incompressible equations of motion and critical point theory to show that the angle of the separating streamline is

$$Tan(\theta) = -3\nu\frac{\Omega_x}{P_x} \tag{5.43}$$

where Ω_x and P_x are the x-derivatives of the vorticity and pressure at the wall. See Perry and Fairlie, Advances in Geophysics **B18**, 299, 1974 and Perry and Fairlie, Journal of Fluid Mechanics **Vol 69**, 657 1975 for a discussion of this problem and an experiment to study boundary layer separation and reattachment.

STANFORD
AERONAUTICS & ASTRONAUTICS

Viscous incompressible Flow near a wall

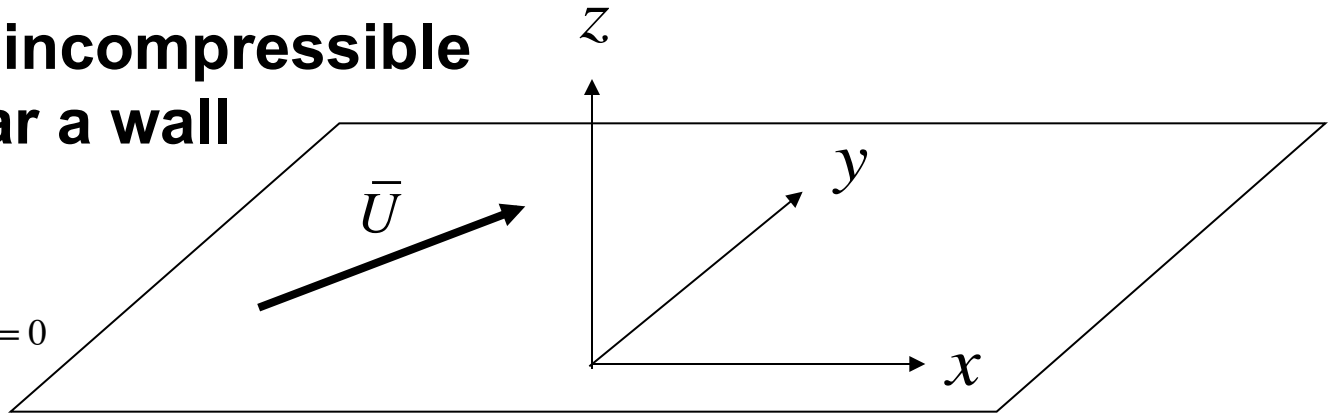

Continuity

$$\nabla \bullet \bar{U} = \frac{\partial U}{\partial x} + \frac{\partial V}{\partial y} + \frac{\partial W}{\partial z} = 0 \Rightarrow \frac{\partial W}{\partial z} = 0$$

Wall viscous stress

$$\frac{\tau_{ij}}{\rho} = \begin{pmatrix} 2\nu\frac{\partial U}{\partial x} & \nu\left(\frac{\partial U}{\partial y}+\frac{\partial V}{\partial x}\right) & \nu\left(\frac{\partial U}{\partial z}+\frac{\partial W}{\partial x}\right) \\ \nu\left(\frac{\partial U}{\partial y}+\frac{\partial V}{\partial x}\right) & 2\nu\frac{\partial V}{\partial y} & \nu\left(\frac{\partial V}{\partial z}+\frac{\partial W}{\partial y}\right) \\ \nu\left(\frac{\partial U}{\partial z}+\frac{\partial W}{\partial x}\right) & \nu\left(\frac{\partial V}{\partial z}+\frac{\partial W}{\partial y}\right) & 2\nu\left(\frac{\partial W}{\partial z}\right) \end{pmatrix} = \begin{pmatrix} 0 & 0 & \nu\left(\frac{\partial U}{\partial z}\right) \\ 0 & 0 & \nu\left(\frac{\partial V}{\partial z}\right) \\ \nu\left(\frac{\partial U}{\partial z}\right) & \nu\left(\frac{\partial V}{\partial z}\right) & 0 \end{pmatrix}$$

Wall viscous traction vector

$$F_i = \frac{\tau_{ij} n_j}{\rho} = \begin{pmatrix} 0 & 0 & \nu\left(\frac{\partial U}{\partial z}\right) \\ 0 & 0 & \nu\left(\frac{\partial V}{\partial z}\right) \\ \nu\left(\frac{\partial U}{\partial z}\right) & \nu\left(\frac{\partial V}{\partial z}\right) & 0 \end{pmatrix} \begin{pmatrix} 0 \\ 0 \\ n_z \end{pmatrix} = \begin{pmatrix} \nu\left(\frac{\partial U}{\partial z}\right) n_z \\ \nu\left(\frac{\partial V}{\partial z}\right) n_z \\ 0 \end{pmatrix} = \begin{pmatrix} F_x \\ F_y \\ 0 \end{pmatrix}$$

Wall viscous traction vector forms a 2-D vector field

STANFORD
AERONAUTICS &
ASTRONAUTICS

Incompressible velocity field near the wall

Expand the velocity field near the wall to second order

$$U = A_{11}x + A_{12}y + A_{13}z + B_{111}x^2 + B_{112}xy + B_{113}xz + B_{122}y^2 + B_{123}yz + B_{133}z^2$$

$$V = A_{21}x + A_{22}y + A_{23}z + B_{211}x^2 + B_{212}xy + B_{213}xz + B_{222}y^2 + B_{223}yz + B_{233}z^2$$

$$W = A_{31}x + A_{32}y + A_{33}z + B_{311}x^2 + B_{312}xy + B_{313}xz + B_{322}y^2 + B_{323}yz + B_{333}z^2$$

$$U = A_{13}z + B_{113}xz + B_{123}yz + B_{133}z^2$$

$$V = A_{23}z + B_{213}xz + B_{223}yz + B_{233}z^2$$

$$W = B_{313}xz + B_{323}yz + B_{333}z^2$$

Near the wall the velocity field is

$$\frac{U}{z} = F_x + B_{113}x + B_{123}y + B_{133}z$$

$$\frac{V}{z} = F_v + B_{213}x + B_{223}y + B_{233}z$$

$$\frac{W}{z} = B_{313}x + B_{323}y + B_{333}z$$

The wall viscous traction vector can be viewed as defining limiting streamlines at the surface.

At a critical point in the wall traction vector field $\left(F_x, F_y\right) = (0,0)$

The streamlines in the neighborhood of a critical point in the wall traction vector field can determined from

$$\frac{dx}{d\tau} = \frac{U}{z} = B_{113}x + B_{123}y + B_{133}z$$

$$\frac{dy}{d\tau} = \frac{V}{z} = B_{213}x + B_{223}y + B_{233}z$$

$$\frac{dz}{d\tau} = \frac{W}{z} = B_{313}x + B_{323}y + B_{333}z$$

Where ?? = zdt is a pseudo-time along a streamline.

STANFORD
AERONAUTICS &
ASTRONAUTICS

Traction vector lines on a sphere. $\sum N - \sum S = 2$

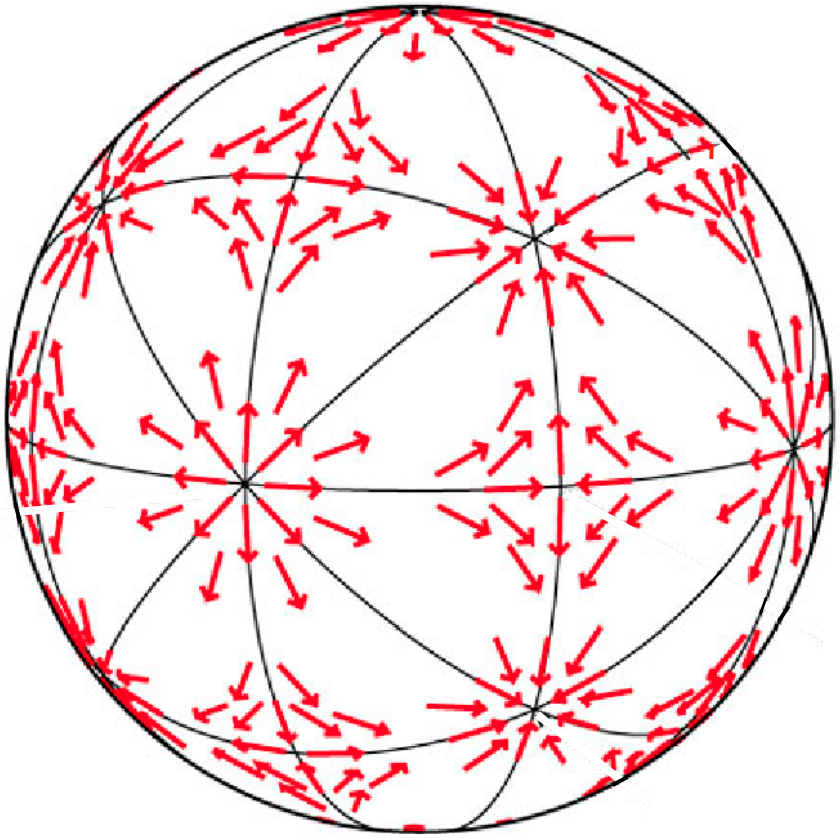

To first order this is a linear system of equations that is solved in terms of exponential functions and only a relatively small number of flow patterns are possible. These patterns are determined by the invariants of the velocity gradient tensor *A*. The invariants are expressed as traces of various powers of *A*. To see this transform the matrix *A*.

$$B_{ik} = M_{in} A_{nm} \bar{M}_{mk}$$

Take the trace.

$$B_{ii} = M_{in} A_{nm} \bar{M}_{mi} = \bar{M}_{mi} M_{in} A_{nm} = \delta_{mn} A_{nm} = A_{mm} .$$

For traces of higher powers the proof of invariance is similar.

$$tr(B^{\alpha}) =$$

$$M_{jn_1} A_{n_1 m_1} \bar{M}_{m_1 j_1} M_{j_1 n_2} A_{n_2 m_2} \bar{M}_{m_2 j_2} \ldots M_{j_{\alpha-1} n_\alpha} A_{n_\alpha m_\alpha} \bar{M}_{m_\alpha j} =$$

$$= tr(A^{\alpha})$$